Purifications have been obtained for compounds from reaction mixtures which either could not have been purified by other means or required a series of steps which greatly reduced yields. The complex *trans*-$[Co(NH_3)_4(NIC)_2]^+$ (NIC = nicotinamide), a minor constituent of the reaction mixture, could only be isolated in trace quantities after a series of tedious chromatographic steps and crystallizations;[16] however, the preparative TLC method allowed separation of the desired product from the reaction mixture in one step. Interestingly the reaction solvent, ethylene glycol, did not interfere with sample application or development (Table I, separation 6).

The isolation procedure[17] for $K[Co(en)(CO_3)_2]$, an important synthetic intermediate, requires many steps, during which hydrolysis of the desired product can occur. Employing the TLC method described here, we can separate the complex from the crude reaction mixture in a single step, greatly reducing the time required for preparation of this material (Table I, separation 7).

The separation of simple geometrical isomers by TLC is not particularly novel, but in the case of [Co(EDDA)(en)]Cl and [Co(EDDA)(pn)]Cl not only were the *u-cis* and *s*-cis isomers of each compound separated but also both sets of isomers were well resolved from one another when a mixture of all four species was chromatographed. The corresponding isomers differ only by a methyl group (Table I, separation 8).

Cobalt complexes of diazotized *N*-acetylhistidine and *N*-acetyltyrosine and related azo dyes have been used as spectrophotometric models for Co^{III}(EDDA)(azoprotein) complexes.[5,18] Formation of these complexes has been followed by spotting the reaction mixture at intervals on plates and then developing. In this way optimal conditions conducive to the formation of these species have been found (Table I, separation 9).

Azo Dye Derivatives. The spectrophotometric characterization of diazotized tyrosine and histidine containing peptides and proteins has been reported.[19,20] Certain inconsistencies appeared when reproduction of some of these modifications were attempted. We have shown[18] that these problems stemmed from the impure model compounds that were originally synthesized.[19] The impurity of these compounds was established by employing this solvent system to separate components of amino acid diazotization reaction mixtures both analytically and preparatively, Table II.

Acknowledgment. This study was supported by NIH Grant GM23081. Excellent technical assistance was provided by Douglas Bower, an NSF Undergraduate Research Participant.

Registry No. Isopropyl alcohol, 67-63-0; TEABC, 15715-58-9.

References and Notes

(1) G. R. Brubaker, D. P. Schaefer, J. H. Worrel, and J. I. Legg, *Coord. Chem. Rev.*, **7**, 161 (1971).
(2) L. F. Druding and G. B. Kaufman, *Coord. Chem. Rev.*, **3**, 409 (1968).
(3) (a) J. A. McClaren, L. A. Dressel, and J. I. Legg, *J. Am. Chem. Soc.*, **98**, 4150 (1976); (b) K. Kawasaki, J. Yoshii, and M. Shibata, *Bull. Chem. Soc. Jpn*, **43**, 3819 (1970); (c) Y. Yoshikawa and K. Yamasaki, *Bull. Chem. Soc. Jpn.*, **45**, 179 (1972).
(4) J. I. Legg, *Coord. Chem. Rev.*, **25**, 103 (1978).
(5) (a) W. I. White and J. I. Legg, *J. Am. Chem. Soc.*, **97**, 3937 (1975); (b) *Bioinorg. Chem.*, **6**, 163 (1976); (c) M. S. Urdea and J. I. Legg, submitted for publication in *Biochemistry*.
(6) U. A. Th. Brinkman, G. De Vries, and R. Kuroda, *J. Chromatogr.*, **85**, 187 (1973).
(7) R. Felici, E. Franco, and M. Cristalli, *J. Chromatogr.*, **90**, 208 (1974).
(8) J. M. Stewart and J. D Young, "Solid Phase Peptide Synthesis", W. H. Freeman and Co., San Francisco, CA, 1969
(9) L. H. Newburn, Ed., "Isco Tables", Instrumentation Specialties Co., Lincoln, NB, 1975.
(10) L. R. Synder and J. J. Kirland, "Modern Liquid Chromatography", Wiley, New York, 1974, pp 264–265.
(11) G. B. Kaufman, B. H. Gump, and B. Stedjee, *J. Chromatogr.*, **121**, 395 (1976).
(12) B. D. Warner, G. H. Boehme, M. S. Urdea, K. H. Pool, and J. I. Legg, manuscript in preparation.
(13) W. E. Keyes and J. I. Legg, *J. Am. Chem. Soc.*, **98**, 4970 (1976).
(14) J. I. Legg and D. W. Cooke, *J. Am. Chem. Soc.*, **89**, 6854 (1967).
(15) W. E. Keyes, Ph.D. Thesis, Washington State University, Pullman, WA, 1976.
(16) T. Wierenga and J. I. Legg, manuscript in preparation.
(17) N. S. Rowan, C. B. Storm, and J. B. Hunt, *Inorg. Chem.*, **17**, 2853 (1978).
(18) M. S. Urdea, B. D. Warner, K. Igi, and J. I. Legg, manuscript in preparation.
(19) M. Tabachnick and H. Sobotka, *J. Biol. Chem.*, **234**, 1726 (1959); **235**, 1051 (1960).
(20) G. F. Fairclough, Jr., and B. L. Vallee, *Biochemistry*, **9**, 4087 (1970).

Contribution from the Centrum voor Oppervlaktescheikunde en Colloidale
Scheikunde, Katholieke Universiteit Leuven, B-3030 Leuven (Heverlee), Belgium

Characterization of $[Ni(en)_x]^{2+}$ (x = 1, 2, 3; en = Ethylenediamine) on the Surface of Montmorillonites

ROBERT A. SCHOONHEYDT,* FIRMIN VELGHE, and JAN B. UYTTERHOEVEN

Received August 24, 1978

The exchange of en complexes of Ni^{2+} on the bidimensional surface of montmorillonite-type minerals gives a mixture of $[Ni(en)_3]^{2+}$, $[Ni(en)_2]^{2+}$, and enH^+ on the surface. These complexes were characterized on the surface by IR and electronic spectroscopy. The relative concentrations depend on the exchange conditions, but the bis complex is preferred. The mono complex disproportionates in the presence of these clay minerals to $[Ni(en)_2]^{2+}$ and $[Ni(H_2O)_6]^{2+}$. The bis complex on the surface is diamagnetic with a characteristic absorption band at 21 500 cm^{-1}. As a consequence the surface is a very weak axial ligand, if a ligand at all. The tris complex decomposes in vacuo below 473 K to the diamagnetic $[Ni(en)_2]^{2+}$ form, which itself is destroyed in vacuo above 473 K. The protonated en molecules decompose below 473 K.

Introduction

The stability of metal uncharged ligand complexes on solid surfaces can be quite different from that in solution.[1,2] Both enhanced stability and destabilization have been found.[2] Thus, the overall formation constant β_2 of $[Cu(en)_2]^{2+}$ on the bidimensional surface of montmorillonite-type clay minerals is $10^{23.1}$ and $10^{21.35}$ on a resin. These numbers are to be compared with the value of 10^{20} in aqueous solution.[1] In the three-dimensional cage network of synthetic faujasites, $[Cu(en)_2]^{2+}$ is destabilized.[2,3] The origin of these effects is not well-known at present. However, it was found that $[Cu(en)_2]^{2+}$ on a Camp Berteau montmorillonite acquired an extra crystal field stabilization energy (CFSE) of 16–23 kJ mol^{-1} with respect to its CFSE in aqueous solution.[4] This was not accompanied by a physically significant change in the Cu–N bonding characteristics except for a slight increase of the covalent

0020-1669/79/1318-1842$01.00/0

character of the out-of-plane π orbital, i.e., the orbital directed toward the surface.[4,5] To gain more insight into this phenomenon of extra stabilization and the effect of the geometry of both the surface and the complex, we extended these studies to the complexes of Ni^{2+} with en, with special attention for $[Ni(en)_3]^{2+}$ as an example of a surface-stabilized octahedral complex. Two layer-type minerals were investigated: Camp Berteau montmorillonite and hectorite. The former has strong lattice absorptions in the UV region, but its higher exchange capacity allowed a study of small complex loadings. The latter allowed a spectroscopic study of the UV region, but because of its smaller exchange capacity it was not suited for detailed studies at low complex loadings.

Experimental Section

Samples. A Camp Berteau montmorillonite and a hectorite were chosen for this study. The lattice compositions are, respectively, $(Si^{4+}{}_4)^{IV}(Al^{3+}{}_{1.46}Mg^{2+}{}_{0.32}Fe^{3+}{}_{0.22})^{VI}O_{10}(OH)_2$ and $(Si^{4+}{}_4)^{IV}$-$(Al^{3+}{}_{0.01}Mg^{2+}{}_{2.71}Li^{+}{}_{0.34})^{VI}O_{10}(OH)_2$. The superscripts IV and VI refer to the tetrahedral and octahedral layers, respectively. The fraction $<0.5\ \mu m$ was separated, brought into the homoionic Na^+ form, freeze-dried, and stored.[6] The cation-exchange capacity (CEC) for Na^+ is 1.00 and 0.70 mequiv g^{-1} for, respectively, Camp Berteau and hectorite.[7,8] Reduced-charge Camp Berteau montmorillonites were prepared by partial exchange of Na^+ with Li^+, followed by heating at 473 K in order to block the Li^+ ions irreversibly in the hexagonal holes of the surface.[9]

Preparation of the Complexes. The complexes were prepared by mixing aqueous solutions of en with aqueous solutions of $Ni(NO_3)_2$, both containing the desired quantities of en and Ni^{2+} to obtain en:Ni ratios of 3, 2, or 1. In the case of the tris complexes, a slight excess of en was added to ascertain the complete formation of the tris complex. The pH of these tris solutions was between 10 and 10.50. Spectra of these solutions were run to verify the nature of the complexes.

Exchange and Analytical Procedures. One percent by weight clay suspensions are placed in dialysis tubing and equilibrated for 24 h at room temperature in an end-over-end shaker with the $[Ni(en)_3]^{2+}$, $[Ni(en)_2]^{2+}$, and $[Ni(en)]^{2+}$ solutions. Typical concentrations are 1 g of clay in 100 mL of H_2O in the dialysis tubing surrounded by 400 mL of exchange solution. By varying the Ni contents of these solutions but respecting the en:Ni ratios, we obtained clays with different exchange levels. For maximum exchange the Ni content of the solution was 1.5 times the CEC of the clay. For the Camp Berteau montmorillonites the pH was not adjusted during exchange. On the hectorites only tris complexes were exchanged, and the pH was kept at its initial value of 10.38 during the exchange reaction by addition of en.

After exchange, the Camp Berteau montmorillonites were either freeze-dried as such or washed with distilled water three times and then freeze-dried. The hectorites were washed three times with en solutions of the same pH as the exchange solution and freeze-dried.

In addition, Ni-containing Camp Berteau montmorillonites with different Ni loadings were prepared by exchange with appropriate $Ni(NO_3)_2$ solutions in a manner analogous to that described for the complex exchanges. The Na^+, Li^+, and Ni^{2+} contents of the clays were determined by atomic absorption spectrometry after dissolution of the minerals in HF. The en content was determined by the Kjeldahl method. These analytical data are shown in Table I together with the sample symbols.

Techniques. Diffuse Reflectance Spectroscopy. Spectra were recorded at room temperature with a Cary 17 instrument equipped with a type II or type I reflectance unit. The samples and the standards (MgO, $Mg(OH)_2$ or the clays in their Na^+ forms) were placed in matching reflectance cells fitted with Suprasil windows.[10] Spectra were recorded *in the regions 2000–210 nm (type I) or 1800–360 nm* (type II) of the samples as such and after evacuation at different temperatures up to 423 K. At each temperature the evacuation time was 48 h. The spectra were digitalized and computer processed to obtain plots of the Kubelka–Munk function against wavenumbers after subtraction of the baseline.[11]

IR Spectroscopy. IR spectra were taken from KBr pellets with 8% by weight of clay on a Beckman IR12 in the regions of 1200–1800 and 2800–3800 cm^{-1}. The reference beam contained a pure KBr pellet.

Table I. Exchangeable Cation and en Contents and the en:Ni Ratios ($\bar{n}$)

sample	amt, mequiv g^{-1} Na(I)	Li(I)	Ni(II)	amt of en, mmol g^{-1}	$\bar{n}$
$Ni(en)_3CB$-1	0.85		0.16	0.32	3.94
$Ni(en)_3CB$-2	0.27 (0.56)[a]		0.59 (0.61)	0.98	3.32
$Ni(en)_3CB$-3	0.06 (0.37)		0.89 (0.91)	1.42	3.19
$Ni(en)_3CB$-4	0.04 (0.36)		1.05 (1.17)	1.75	3.32
$Ni(en)_3CB$-5	0.15 (1.00)		1.03 (1.70)	1.70	3.30
$Ni(en)_3RCB$-1	0.22	0.44	0.36	0.58	3.19
$Ni(en)_3RCB$-2	0.10	0.19	0.81	1.23	3.03
$Ni(en)_2CB$	0.23		1.25	1.46	2.34
Ni(en)CB	0.23		1.28	1.40	1.40
NiCB-1	0.59		0.43		
NiCB-2	0.06		1.31		
$Ni(en)_3H$-1	0.66		0.42	0.65	3.09
$Ni(en)_3H$-2	0.07		0.94	1.28	2.72

[a] The numbers between parentheses are the exchangeable cation contents without washing.

X-ray Diffraction. X-ray diffraction patterns of the Camp Berteau montmorillonites were obtained with a Debye–Scherrer camera (ϕ 114.6 mm) by using Straumanis' method on the clays in their initial state and after stepwise evacuation up to 533 K.[12] The evacuation time at each temperature was 48 h. While under vacuum, the clays were brought into a Lindemann capillary (ϕ 0.5 mm), which was sealed off for X-ray investigation. The radiation was Cu Kα (λ 0.154 18 nm). The diffraction patterns of the hectorites were recorded on a Seifert-Scintag PAD III apparatus. The *d* 001 spacing was obtained from a computer fit of the position of the maximum of the first reflection.

Desorption. Desorptions were performed either stepwise or continuously. In the first case ~100 mg of complex-loaded clay was placed in an Al-foil sample holder and hooked on a calibrated spring balance. The samples were evacuated and heated under dynamic vacuum ($p < 1.351 \times 10^{-2}$ Pa) in a stepwise manner up to 623 K. After each step the sample was allowed to equilibrate until constant weight. The sensitivity of the spring was 0.5 mg mm^{-1}, and the estimated error on the total weight loss was less than 5%. Continuous desorptions were run in a Mettler thermobalance under N_2 flow with a heating rate of 0.066 K s^{-1} from room temperature up to 873 K.

Adsorption. About 100 mg of Ni(II) containing CB montmorillonite was placed in a vacuum reflectance cell and the spectrum recorded as described previously. After evacuation at room temperature, en was allowed to adsorb in slugs of about 0.5 mol of en/mol of Ni^{2+}. The amount of en adsorbed was monitored by a calibrated volume between the sample containing reflectance cell and the reservoir with en. After addition of each slug the equilibration time was 48 h prior to recording the spectrum. After the adsorption of 3 mol of en/mol of Ni^{2+} the sample was equilibrated in en vapor at room temperature and the spectrum recorded again.

Results

The exchange of complexes of the type $[Ni(en)_x]^{2+}$ ($x = 1, 2, 3$) involves a complicated set of reactions. The evidence is derived from the analytical data of Table I. In no case is the solution en:Ni ratio recovered on the surface. The different ratios obtained on Camp Berteau montmorillonites and hectorites and the dependence of the en:Ni ratio on the exchange level for both types of minerals indicate the predominant role of the exchange conditions on the nature of the surface species. It is anticipated that the surface is covered both with $[Ni(en)_x]^{2+}$ complexes and protonated en molecules. The spectroscopic techniques allow their identification.

Reflectance Spectroscopy. The reflectance spectra of the complexes on the clay surfaces reveal three types of bands: (i) N–H, C–H, and OH vibrational overtones and combinations; (ii) d–d transitions; (iii) charge-transfer bands. Spectra of $[Ni(en)_3]^{2+}$ on hectorite are shown in Figure 1. Thus, $(\nu + \delta)(H_2O)$ is at 5226 cm^{-1}, $2\nu(CH)$ between 5600 and 5900 cm^{-1}, $2\nu(NH)$ at 6530 cm^{-1}, $2\nu(H_2O)$ at 6872 and 7115 cm^{-1}, and 2ν(lattice OH) at 7225 cm^{-1}. The transitions within the d shell of Ni^{2+} are present as broad bands at 11 000

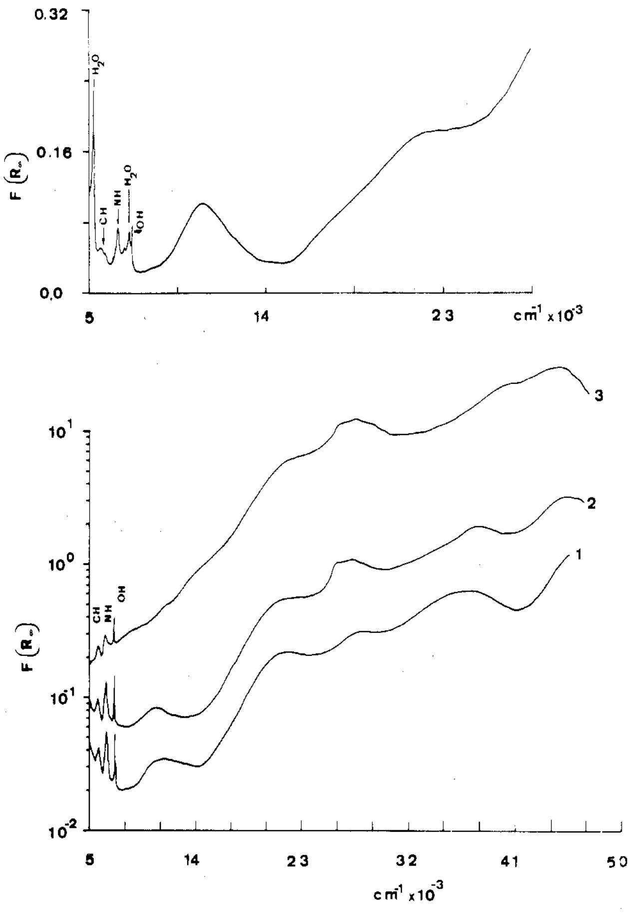

Figure 1. Reflectance spectra of $Ni(en)_3H$. Top: $Ni(en)_3H$-2. Bottom: 1, $Ni(en)_3H$-1 evacuated at 295 K; 2, $Ni(en)_3H$-1 evacuated at 373 K; 3, $Ni(en)_3H$-1 evacuated at 473 K. The scales of 2 and 3 are shifted upward by factors of 2 and 10, respectively, with respect to the indicated scale.

and 21 500 cm^{-1} with shoulders around 18 000 and 27 000 cm^{-1}. The bands at 11 000, 18 000, and 27 000 cm^{-1} are easily recognized as the d–d transitions of Ni^{2+} in the octahedral environment of three en molecules.[13,14] The 21 500-cm^{-1} band is typical for planar, diamagnetic $[Ni(en)_2]^{2+}$.[15-18] The ratio of the octahedral band intensities to the planar band intensities depends on the ion-exchange level, the exchange conditions, and the sample treatment. The water bands are almost completely eliminated after evacuation at room temperature. The 11 000-cm^{-1} band of $Ni(en)_3{}^{2+}$ is eliminated at 473 K. In the course of the evacuation process, spectral changes are observed in the 27 000-cm^{-1} region (Figure 1) due to the elimination of the $Ni(en)_3{}^{2+}$ band and the appearance of a clay lattice or impurity absorption. This was verified by recording the spectra against hydrated Na^+-hectorite. The same technique allowed the identification of the other bands in the UV region. Thus, the band around 36 500 cm^{-1}, moving toward 40 000 cm^{-1} upon heating of the sample, is also a lattice absorption. The band tail, starting at 44 000 cm^{-1} in the room-temperature spectrum, becomes a fully developed band with a maximum around 44 000 cm^{-1} after evacuation at 473 K. It remains in the spectrum when recorded against Na^+-hectorite. We assign it as a N→Ni charge-transfer band. On the Camp Berteau montmorillonites, exchanged without rigorous pH control at pH 10.30, the planar:octahedral ratio is consistently higher than on the hectorites. Washing the samples with distilled water after the exchange reaction also promotes the formation of the diamagnetic bis complex. Finally, in identical exchange conditions, the planar:octahedral ratio is higher at low-exchange levels than at high loadings of the surface.

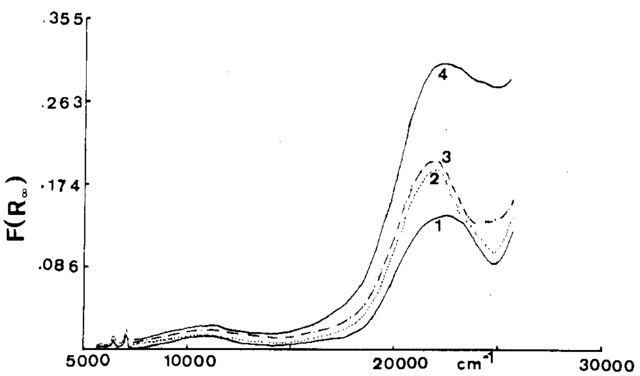

Figure 2. Reflectance spectra of $Ni(en)_2CB$: 1, hydrated; 2, evacuated at 376 K; 3, evacuated at 298 K; 4, evacuated at 423 K.

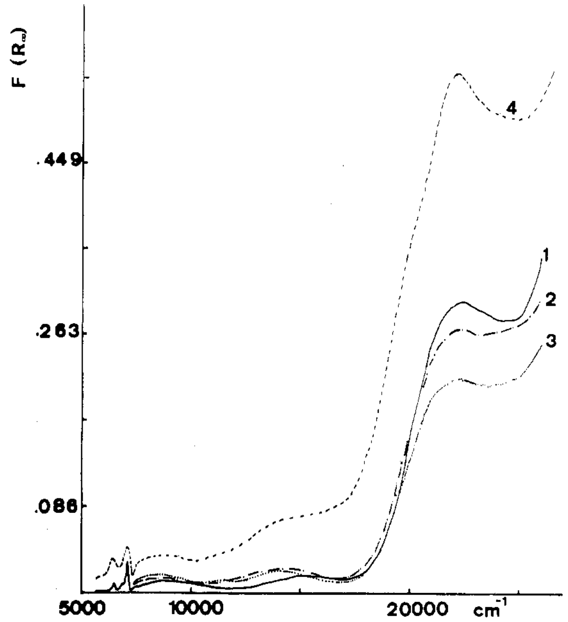

Figure 3. Reflectance spectra of $Ni(en)CB$: 1, hydrated; 2, evacuated at 298 K; 3, evacuated at 373 K; 4, evacuated at 411 K.

We have ascertained that the diamagnetic bis complex was really exchanged on the surface and not only a product of the experimental procedure by taking spectra of aqueous suspensions of $Ni(en)_3CB$-1, $Ni(en)_3H$-1 and $Ni(en)_3H$-2 immediately after exchange with no residual Ni in the supernatant. In every case the 21 500-cm^{-1} band was present besides those of $[Ni(en)_3]^{2+}$. Also, the nature of the outgoing cation had no influence on its presence: a Mg^{2+}-hectorite, loaded with $[Ni(en)_3]^{2+}$ solutions up to 40% of its CEC, gave spectra typical for the simultaneous presence of bis and tris complexes.

Figure 2 shows spectra of $Ni(en)_2CB$. The presence of a band at 10 800 cm^{-1} and one around 22 000 cm^{-1} indicates the simultaneous presence of octahedral and planar Ni^{2+} complexes. The latter is the predominant species, and its surface concentration increases upon thermal evacuation at the expense of the octahedral Ni^{2+} complex. The reflectance spectra of $Ni(en)CB$ (Figure 3) are different in that, besides the 22 000-cm^{-1} band, two bands are present at 8500 and 15 500 cm^{-1}. They indicate the presence of $Ni(H_2O)_6{}^{2+}$ on the surface.[13,14] Upon thermal evacuation of the sample, the 15 500-cm^{-1} band shifts to ~14 000 cm^{-1}, while the 8500-cm^{-1} band flattens and becomes ill-defined. This 14 000-cm^{-1} band may indicate partial dehydration of $[Ni(H_2O)_6]^{2+}$ to the tetrahedral-like species $[(O_l)_3Ni{-}OH_2]^{2+}$ where O_l means a lattice oxygen.[10]

Infrared Spectroscopy. Representative spectra for $Ni(en)_3$-exchanged clays are collected in Figure 4. The lattice

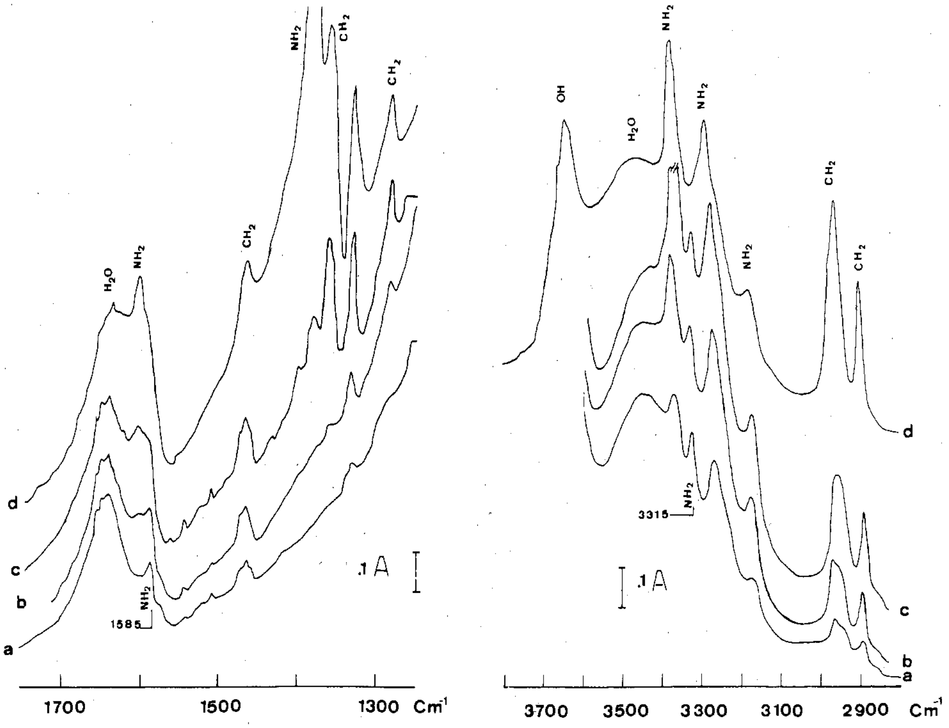

Figure 4. IR spectra of $Ni(en)_3CB$: a, $Ni(en)_3CB$-2; b, $Ni(en)_3CB$-3; c, $Ni(en)_3CB$-4; d, $Ni(en)_3CB$-5.

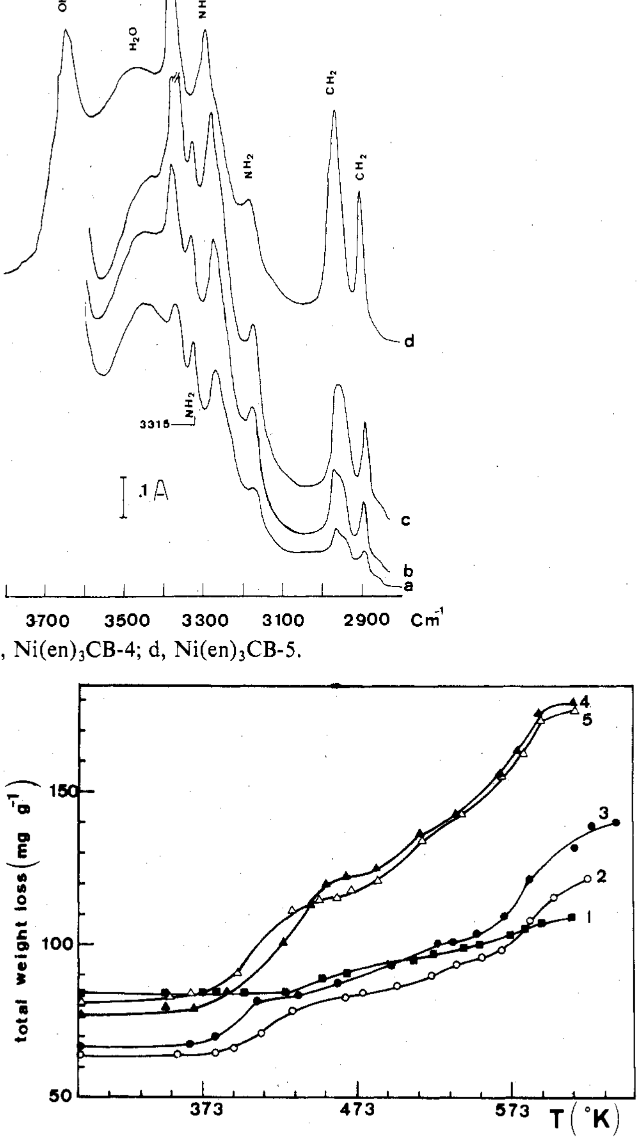

Figure 5. Total weight loss curves in vacuo: 1, $Ni(en)_3CB$-1; 2, $Ni(en)_3CB$-2; 3, $Ni(en)_3CB$-3; 4, $Ni(en)_3CB$-4; 5, $Ni(en)_3CB$-5.

Table II. *d* 001 Distances (nm) for the $[Ni(en)_3]^{2+}$-, $[Ni(en)_2]^{2+}$-, and $[Ni(en)]^{2+}$-Exchanged Clays

		temp, K			
sample	hydrated	298	373	448	533
$Ni(en)_3CB$-1	1.194	1.174	1.009	1.024	0.980
$Ni(en)_3CB$-2	1.288	1.298	1.286	1.276	1.260
$Ni(en)_3CB$-3	1.335	1.332	1.339	1.277	1.280
$Ni(en)_3CB$-4	1.396	1.398	1.354	1.281	1.272
$Ni(en)_3CB$-5	1.425	1.392	1.370	1.319	1.242
$Ni(en)_3RCB$-1	1.181	1.151		1.169	
$Ni(en)_3RCB$-2	1.385	1.370	1.349	1.345	
$Ni(en)_2CB$	1.345		1.337	1.302	1.264
$Ni(en)CB$	1.329		1.277	1.235	1.249
$Ni(en)_3H$-1	1.326				
$Ni(en)_3H$-2	1.390				

hydroxyls of CB montmorillonite absorb around 3630 cm^{-1}. Broad water bands are found with maxima around 3460 and 1640 cm^{-1}, the latter showing considerable structure. The absorption tail below 1300 cm^{-1} is the onset of the lattice vibrations. All of the other bands are due to en molecules. The assignments given on Figure 4 are derived from the work of Powell and Sheppard[19] and Berg and Rasmussen.[20] The N–H stretching band at 3315 cm^{-1} (3300 cm^{-1} for hectorites) and the NH-deformation band at 1585 cm^{-1} are typical for $[Ni(en)_2]^{2+}$. They are particularly well resolved at low exchange levels, but not detectable at maximum exchange levels. In the latter case, the spectrum is characteristic for $[Ni(en)_3]^{2+}$. The decreasing bis:tris ratio with increasing exchange levels is in accordance with the reflectance spectroscopic data. This is also the case for the other samples studied. In no case did we find clear evidence for the presence of protonated en molecules. It is possible that the weak bands between 1500 and 1550 cm^{-1} visible at low loadings in Figure 4 are due to the $-NH_3^+$ groups.

Thermostability of $[Ni(en)_x]^{2+}$ on the Clay Surface. Representative examples of weight loss curves, measured on spring balances, are shown in Figure 5. Three phenomena occur: desorption of water, desorption of en, and dehydroxylation of lattice hydroxyl groups. It is generally accepted that dehydroxylation does not start below 673 K.[21] The curves in Figure 5 represent then the two other processes. The reflectance spectra in Figure 1 showed the nearly complete elimination of physisorbed H_2O at room temperature. This is confirmed in Figure 5 by the weight loss accompanying the evacuation at room temperature. The weight loss starting at ~383 K and leveling off around 623 K is due to desorption of en. The amount agrees quantitatively with that determined by Kjeldahl analysis. This is taken as indirect evidence for desorption of en as such. One can distinguish three regions: desorption below 473 K, desorption above 553 K, and an intermediate region. The first region can be ascribed to the decomposition of $Ni(en)_3^{2+}$ to $Ni(en)_2^{2+}$ in agreement with the reflectance spectroscopic data and the literature on the decomposition of $Ni(en)_3X_2$.[22] Also protonated en molecules decompose in that region.[23] This process is accompanied by a decrease of the *d* 001 distances (Table II) into the range 1.242–1.280 mm, typical for planar complexes between the clay layers.[4] A quantitative separation of the three desorption regions of Figure 5 is not believed to be physically meaningful. This is the more so, as only two en desorption regions (below and above 578 K) were separated in the thermobalance under N_2 flow with a rate of temperature increase of 0.066 K s^{-1}. Also,

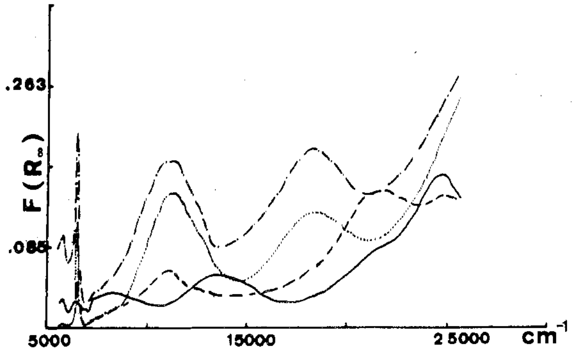

Figure 6. Reflectance spectra of NiCB after adsorption of en: —, en:Ni = 0.24; ---, en:Ni = 1.0; ···, en:Ni = 1.99; —·—, en:Ni = 3.22.

Table III. Initial Composition (mmol dm^{-3}) of the Exchange Solution at pH 10.38

	$Ni(en)_3H$-1	$Ni(en)_3H$-2
en	0.79	0.79
enH^+	0.208	0.208
enH_2^{2+}	6.73×10^{-5}	6.73×10^{-5}
Ni^{2+}	7×10^{-9}	2.10×10^{-9}
$Ni(en)^{2+}$	1.6×10^{-4}	3.17×10^{-5}
$Ni(en)_2^{2+}$	9.65×10^{-2}	2.89×10^{-2}
$Ni(en)_3^{2+}$	1.16	0.346

in this case, the separation could not be quantified.

Adsorption of Gaseous en on NiCB. Figure 6 shows the reflectance spectra of NiCB-1 at different loadings of en. The initial spectrum is that of $[Ni(H_2O)_6]^{2+}$ with bands at 8250 cm^{-1} and in the range 13 000–15 000 cm^{-1}. The first slug of en produces a new band at 21 500 cm^{-1}, typical for diamagnetic planar $[Ni(en)_2]^{2+}$. It reaches its maximum intensity at en:Ni = 0.75. At higher loadings of en, $[Ni(en)_3]^{2-}$ becomes the predominant species on the surface as evidenced by the bands at 11 000 and 18 200 cm^{-1}. Adsorption of dry, gaseous en on a NiCB with only 0.35 mequiv g^{-1} of Ni^{2+} produced the same band systems. However the 21 500-cm^{-1} band was persistent up to saturation of the sample with en. The comparison of these two experiments establishes the heterogeneity of the surface. At low Ni contents, all the Ni^{2+} ions are located in the interlamellar space where it is more difficult to form tris complexes than on the external surface.

Discussion

The presence of tris and bis complexes of Ni^{2+} with en and of enH^+ on the surface was shown directly by spectroscopy and quantitative desorption studies. Their presence on the surface can be anticipated qualitatively from the composition of the initial exchange solution, shown in Table III for $Ni(en)_3H$-1 and $Ni(en)_3H$-2. These data indicate that, with respect to the initial concentration of $[Ni(en)_3]^{2+}$, nonnegligible amounts of enH^+ and $[Ni(en)_2(H_2O)_2]^{2+}$ are present. The ratio tris:bis is constant, but the ratio en:Ni increases in the solution for small exchange levels because they were brought to the same pH by addition of en. Thus the decrease of the en:Ni ratio on the surface with increasing exchange levels translates the decreasing contribution of enH^+ to the ion-exchange process. The three different cations are not exchanged with the same selectivity. Indeed, although the tris:bis ratio in the initial solutions is constant, it increases with increasing exchange level on the surface, suggesting that at low loadings the selectivity for the bis complex is higher than for the tris complex.

Other evidence for the preference of the surface for $[Ni(en)_2]^{2+}$ comes from the exchanges with solutions of en:Ni = 1 and 2 and the adsorption of gaseous en. Solutions with en:Ni ratios of 2 contain the three types of complexes, yet only $[Ni(en)_2]^{2+}$ and $[Ni(en)_3]^{2+}$ are found on the surface. With en:Ni = 1, no mono complex was on the surface, only $[Ni(en)_2]^{2+}$ and $[Ni(H_2O)_6]^{2+}$. We have to assume a disproportionation reaction:

$$2[Ni(en)(H_2O)_4]^{2+} \rightarrow [Ni(H_2O)_6]^{2+} + [Ni(en)_2]^{2+} + 2H_2O$$

The adsorption of en is a two-step process:

$$[Ni(H_2O)_6]^{2+} \xrightarrow{en} [Ni(en)_2]^{2+} \xrightarrow{en} [Ni(en)_3]^{2+}$$

The last two cases are analogous to the behavior of the en complexes of Cu^{2+}.[4] However, the exchange of the bis complex of Ni^{2+} is more than just an exchange reaction. It is accompanied by (i) the loss of two water molecules,

$$[Ni(en)_2(H_2O)_2]^{2+} \rightarrow [Ni(en)_2]^{2+} + 2H_2O$$

(ii) the conversion of Ni^{2+} from the paramagnetic to the diamagnetic state, and (iii) a shortening of the equatorial Ni–N distance from 0.212 nm for high-spin Ni^{2+} to ~0.185 nm for low-spin Ni^{2+}.[24-27] A diamagnetic, planar Ni^{2+} complex is formed when the axial ligand field strength is very weak with respect to the strength of the equatorial ligands.[17,28,29] Thus the clay surface has a weak coordinating power with respect to the strength of the en ligands. It is possible that a surface–ligand interaction exists, which affects the complex properties. One should then expect some changes in the position of the charge-transfer bands with respect to their position in aqueous solutions. The shift of the N → Ni charge-transfer band to lower wavenumbers upon elimination of physisorbed water confirms this statement.

Acknowledgment. We acknowledge support for this research from the Belgian Government (Staatssekretariaat voor Wetenschapsbeleid). R.A.S. is indebted to the NFWO (Belgium) for a research position as "Bevoegdverklaard Navorser". F.V. acknowledges the IWONL for a Ph.D. grant. The authors thank F. Pelgrims and R. Baerts for technical assistance.

Registry No. Montmorillonite, 1318-93-0; $[Ni(en)_3]^{2+}$, 15390-99-5; $[Ni(en)_2]^{2+}$, 15390-98-4; enH^+, 26265-69-0; $[Ni(H_2O)_6]^{2+}$, 15365-79-4.

References and Notes

(1) A. Maes, P. Peigneur, and A. Cremers, *J. Chem. Soc., Faraday Trans. 1*, **74**, 182 (1978).
(2) P. Peigneur, Ph.D. Thesis, Faculty of Agronomy, K. U. Leuven, Belgium, 1976.
(3) P. Peigneur, J. H. Lunsford, W. De Wilde, and R. A. Schoonheydt, *J. Phys. Chem.*, **81**, 1179 (1977).
(4) F. Velghe, R. A. Schoonheydt, J. B. Uytterhoeven, P. Peigneur, and J. H. Lunsford, *J. Phys. Chem.*, **81**, 1187 (1977).
(5) R. A. Schoonheydt, *J. Phys. Chem.*, **82**, 497 (1978).
(6) A. Cremers and H. C. Thomas, *J. Phys. Chem.*, **70**, 3229 (1966).
(7) A. Maes, P. Peigneur, and A. Cremers, *Proc. Int. Clay Conf.*, 319 (1975).
(8) A. Maes and A. Cremers, *J. Chem. Soc., Faraday Trans 1*, **73**, 1807 (1977).
(9) U. Hofmann and R. Klemen, *Z. Anorg. Allg. Chem.*, **262**, 95 (1950).
(10) F. Velghe, R. A. Schoonheydt, and J. B. Uytterhoeven, *Clays Clay Miner.*, **25**, 375 (1977).
(11) G. Kortüm, "Reflectance Spectroscopy", Springer Verlag, West Berlin, 1969, Chapter 4.
(12) H. S. Peiser, H. P. Rooksby, and A. J. C. Wilson, "X-ray Diffraction by Polycrystalline Materials", J. Wright and Sons, Bristol, England, 1955.
(13) A. B. P. Lever, "Inorganic Electronic Spectroscopy", Elsevier, Amsterdam, 1968.
(14) E. König, *Struct. Bonding (Berlin)*, **9**, 175 (1971).
(15) Ch. K. Jørgensen, *Acta Chem. Scand.*, **11**, 399 (1957).
(16) A. B. P. Lever, J. Lewis, and R. S. Nyholm, *J. Chem. Soc.*, 2552 (1963).
(17) A. B. P. Lever, *Coord. Chem. Rev.*, **3**, 119 (1968).
(18) C. J. Ballhausen and A. D. Liehr, *J. Am. Chem. Soc.*, **81**, 538 (1959).
(19) D. B. Powell and N. Sheppard, *Spectrochim. Acta*, **17**, 68 (1961).
(20) R. W. Berg and K. Rasmussen, *Spectrochim. Acta, Sect. A*, **30**, 1881 (1974).
(21) R. E. Grim, "Clay Mineralogy", McGraw-Hill, New York, 1968, Chapter 9.
(22) W. W. Wendlandt and J. P. Smith, "The Thermal Properties of Transition Metal Ammine Complexes", Elsevier, Amsterdam, 1967.

(23) P. Cloos and R. D. Laura, *Clays Clay Miner.*, **20**, 259 (1972).
(24) L. Y. Martin, C. R. Sperati, and D. H. Busch, *J. Am. Chem. Soc.*, **99**, 2968 (1977).
(25) M. C. Weiss, G. Gordon, and V. L. Goedken, *Inorg. Chem.*, **16**, 305 (1977).
(26) M.-U. Haque, C. N. Caughlan, and K. Emerson, *Inorg. Chem.*, **9**, 2421 (1970).
(27) L. N. Surink and M. Atoji, *Acta Crystallogr.*, **13**, 639 (1960).
(28) J. C. Donini, B. R. Hollebone, and A. B. P. Lever, *J. Am. Chem. Soc.*, **93**, 6455 (1971).
(29) J. C. Donini, B. R. Hollebone, G. London, A. B. P. Lever, and J. C. Hempel, *Inorg. Chem.*, **14**, 455 (1975).

Contribution from the Department of Chemistry,
University of Nebraska, Lincoln, Nebraska 68588

Distortions of the Coordination Polyhedron in High-Spin Manganese(III) Complexes. 2. Crystal Structure of Thiocyanatobis(acetylacetonato)manganese(III)[1-4]

B. RAY STULTS, ROBERTA O. DAY, ROBERT S. MARIANELLI, and VICTOR W. DAY*[5]

Received February 23, 1977

The crystal structure of thiocyanatobis(acetylacetonato)manganese(III), $Mn(O_2C_5H_7)_2(NCS)$, has been determined by single-crystal X-ray diffraction techniques and refined anisotropically for all nonhydrogen atoms by full-matrix least-squares techniques to $R_1 = 0.057$ and $R_2 = 0.061$ by using 1917 independent diffractometer-recorded reflections (Nb-filtered Mo K_α radiation and θ–2θ scans) having $2\theta_{MoK\alpha} < 55°$ and $I > 2\sigma(I)$. The compound crystallizes in the uniquely determined centrosymmetric orthorhombic space group *Pbca* with eight molecules in a unit cell of dimensions $a = 13.422$ (2) Å, $b = 14.519$ (3) Å, and $c = 13.763$ (3) Å ($\rho_{calcd} = 1.541$ g/cm^3, $\rho_{obsd} = 1.540$ g/cm^3). Each thiocyanato ligand bridges two adjacent quasi-planar $Mn(acac)_2^+$ groups in the three-dimensional lattice by using the glide operator perpendicular to the $\vec{c}$ axis of the unit cell to generate infinite chains of octahedral Mn(III) subunits along the $\vec{a}$ axis. The octahedral coordination polyhedron is tetragonally elongated and approximates idealized C_{4v} symmetry with the trans-coordinated thiocyanato nitrogen and sulfur atoms on the pseudo-fourfold axis. The four "short" Mn–O bonds have average lengths of 1.912 (4) Å while the two long trans Mn–N and Mn–S′ bonds to the ends of bridging thiocyanato ligands have lengths of 2.189 (5) and 2.880 (2) Å, respectively. The dissimilarity of the two ends of the thiocyanato ligand has a pronounced effect on the Mn coordination geometry in this complex. The Mn atom is displaced by 0.12 Å from the mean plane of the quasi-square of four coordinated oxygen atoms toward the coordinated thiocyanato nitrogen atom.

Introduction

This is the second of three papers[1] dealing with the coordination chemistry for a series of high-spin manganese(III) acetylacetonato (acac) complexes. The first paper described the synthesis and characterization of a series of compounds having the formulations $Mn(acac)_2(X)$ and $Mn(acac)_2(X)(B)$, where X is a mononegative anionic ligand such as N_3^-, NCS^-, or Cl^- and B is a neutral Lewis base such as pyridine or methanol. These compounds serve as useful synthetic intermediates for manganese(III) porphyrins and provide a simple high-yield procedure for preparing these interesting compounds in pure form. The solid-state structure of $Mn(acac)_2(N_3)$, **1**, reported in the first paper of this series[1] revealed several interesting features of high-spin Mn(III) and azide ligand coordination chemistry. Each azide ligand in crystals of this compound symmetrically bridges (through its first and third nitrogen atoms) two adjacent $Mn(acac)_2^+$ groups in the three-dimensional lattice to produce infinite chains of octahedral Mn(III) subunits. Each of these octahedral coordination polyhedra is tetragonally elongated and approximates idealized D_{4h} symmetry with four "short" Mn–O and two "long" Mn–N bonds. Since the azide ligand produced symmetrical bridges between Mn atoms in the solid state to give regularly elongated octahedral species with identical trans Mn–N bonds, it was of interest to characterize the closely related complex $Mn(acac)_2(NCS)$ (**2**), in which the azide ligand has been replaced by the less symmetrical thiocyanate ligand. Other properties[1] also did not exclude the possibility of a five-coordinate Mn in this complex. Although each of the thiocyanate ligands in **2** also bridges adjacent $Mn(acac)_2^+$ groups in the three-dimensional lattice to produce infinite chains of octahedral Mn(III) subunits, the dissimilarity of the two ends of the thiocyanate ligand have a significant effect on the coordination geometry observed for the Mn atom.

Experimental Section

Large, well-shaped single crystals of thiocyanatobis(acetylacetonato)manganese(III), prepared as previously reported,[1,6] may be grown from a saturated solution of methanol or acetonitrile by slow solvent evaporation at 5 °C. Single crystals (as shown by X-ray photographs) grown from methanol are rapidly converted into a powder at room temperature which analyzes as $Mn(O_2C_5H_7)_2(NCS)$, **2**. These results are presumably due to the loss of (coordinated or lattice) methanol from the original crystalline material. Crystals grown from acetonitrile proved to be unsolvated and stable; they were used for subsequent crystallographic studies.

Precession photographs used to determine a preliminary set of lattice constants and the probable space group indicated orthorhombic, *mmm*, symmetry. The observed systematically absent reflections were those uniquely required by the centrosymmetric space group *Pbca* (D_{2h}^{15}, No. 61).[7] This choice was fully supported by the negative results of sensitive tests for piezoelectricity[8] and by all stages of the subsequent structure determination.

An approximately cube-shaped crystalline specimen 0.50 mm on an edge was cut from a large single crystal and ground to a sphere 0.44 mm in diameter before being glued to the inner wall of a sealed thin-walled glass capillary. The lattice constants obtained from this specimen as previously described[1] by using 15 high-angle reflections ($2\theta_{MoK\bar{\alpha}} > 30°$) and Nb-filtered Mo $K\bar{\alpha}$ radiation (λ 0.710 69 Å) on a Syntex $P\bar{1}$ Autodiffractometer at 20 ± 1 °C are $a = 13.422$ (2), $b = 14.519$ (3), and $c = 13.763$ (3) Å. A unit cell with these dimensions containing eight $Mn(acac)_2(NCS)$ formula units has a calculated density of 1.541 g cm^{-3}, which is in excellent agreement with the observed density of 1.540 g cm^{-3} measured by flotation in a carbon tetrachloride/hexane solution.

Intensities were measured by using Nb-filtered Mo $K\bar{\alpha}$ radiation and θ–2θ scans with a 3° takeoff angle and a normal-focus X-ray tube. A scan rate of 3°/min was employed for scans between 2θ settings 1.0° above and below the calculated $K\alpha$ doublet ($\lambda_{K\alpha_1}$ 0.709 26 Å and $\lambda_{K\alpha_2}$ 0.713 54 Å) values for each reflection. Background counts, each lasting for half the total scan time, were taken at both ends of the scan range. A total of 3076 independent reflections having $2\theta_{MoK\bar{\alpha}} < 55°$ (the equivalent of one limiting Cu $K\bar{\alpha}$ sphere) were measured in two concentric shells of increasing 2θ containing approximately 1550 reflections each. Six standard reflections, measured every 200 reflections as a monitor for disalignment and/or deterioration of the crystal, gave no indication of either.

The linear absorption coefficient of the crystal for Mo $K\bar{\alpha}$ radiation is 1.186 mm^{-1},[9] yielding a μr of 0.26 for the spherical specimen used for intensity measurements. Since variable absorption for a spherical

0020-1669/79/1318-1847$01.00/0